



# Determining equilibrium partition coefficients between lipid/protein and polydimethylsiloxane for highly hydrophobic organic contaminants using preloaded disks



Yuanyuan Pei<sup>a,b,c</sup>, Huizhen Li<sup>b</sup>, Jing You<sup>b,\*</sup>

<sup>a</sup> State Key Laboratory of Organic Geochemistry, Guangzhou Institute of Geochemistry, Chinese Academy of Sciences, Guangzhou 510640, China

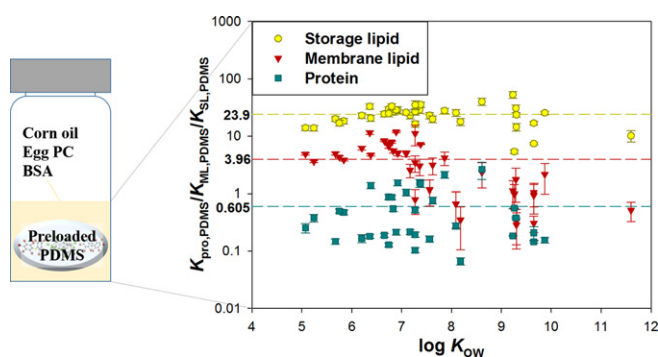
<sup>b</sup> School of Environment, Guangzhou Key Laboratory of Environmental Exposure and Health, and Guangdong Key Laboratory of Environmental Pollution and Health, Jinan University, Guangzhou 510632, China

<sup>c</sup> University of Chinese Academy of Sciences, Beijing 100049, China

## HIGHLIGHTS

- Preloaded PDMS disks showed viable loading efficiency for hydrophobic compounds.
- Partition coefficients ( $K_{SL,PDMS}$ ,  $K_{ML,PDMS}$  and  $K_{pro,PDMS}$ ) were determined.
- Partitioning between biological phases and PDMS was independent of hydrophobicity.
- Pseudo-equilibrium explained different  $K_{pro,PDMS}$  for compounds with  $\log K_{OW} > 9$ .
- The SL had the highest sorption capacity, followed by ML and protein.

## GRAPHICAL ABSTRACT



## ARTICLE INFO

### Article history:

Received 16 March 2017

Received in revised form 14 April 2017

Accepted 16 April 2017

Available online 24 April 2017

Editor: Jay Gan

### Keywords:

Highly hydrophobic organic contaminants

Partition coefficients

Preloaded PDMS

Lipid

Protein

Bioaccumulation

## ABSTRACT

Bioaccumulation of hydrophobic organic contaminants is of great concern and understanding their partitioning to biological phases is crucial for estimating their bioaccumulation potential. The estimation, however, was of large uncertainty for highly hydrophobic organic contaminants (HHOCs) with  $\log K_{OW} > 9$  due to the challenge of quantifying their water concentrations. In the present study, partition coefficients between polydimethylsiloxane (PDMS) and storage lipid ( $K_{SL,PDMS}$ ), membrane lipid ( $K_{ML,PDMS}$ ) and protein ( $K_{pro,PDMS}$ ) were measured for 21 polychlorinated biphenyls (PCBs), 14 polybrominated diphenyl ethers (PBDEs), dechlorane plus (DP) and decabromodiphenyl ethane (DBDPE), covering  $\log K_{OW}$  from 5.07 to 11.6, using a preloaded PDMS depletion method. The values of  $K_{SL,PDMS}$ ,  $K_{ML,PDMS}$  and  $K_{pro,PDMS}$  were in the ranges of 5.36–52.5, 0.286–11.8 and 0.067–2.62 g/g, respectively, being relatively constant although their  $K_{OW}$  values extend more than six orders of magnitude. The relative sorption capacity of the biological phases showed storage lipid was the dominant sorption phase in biota, followed by membrane lipid and protein was the lowest. The  $K_{PDMS,pro}$  values of the compounds with  $\log K_{OW} < 9$  were similar (0.382–14.9 g/g) regardless of the thickness of preloaded PDMS disks (58–209  $\mu\text{m}$ ). For HHOCs, however,  $K_{PDMS,pro}$  values dropped when thinner PDMS disks were used, as a result of slow diffusion of HHOCs in PDMS. The  $K_{PDMS,pro}$  values of HHOCs measured by 58- $\mu\text{m}$  PDMS disks ranged from 1.78 to 6.85 g/g, which was consistent with compounds with  $\log K_{OW} < 9$ . This validated that partition coefficients between PDMS

\* Corresponding author.

E-mail address: [yujing@jnu.edu.cn](mailto:yujing@jnu.edu.cn) (J. You).

and biological phases were independent of chemical hydrophobicity, showing the advantage of using PDMS-based methods to directly estimate bioaccumulation potential of HHOCs.

© 2017 Elsevier B.V. All rights reserved.

## 1. Introduction

Halogenated hydrocarbons, like polychlorinated biphenyls (PCBs) and polybrominated diphenyl ethers (PBDEs) were historically used and are still of great concern nowadays owing to their persistence, bioaccumulation and toxicity (Hites, 2004; Diamond et al., 2010). The restriction on penta- and octa-BDEs promoted the use of highly hydrophobic organic contaminants (HHOCs) as flame retardants, including decabrominated diphenyl ether (BDE-209), dechlorane plus (DP) and decabromodiphenyl ethane (DBDPE) (Wang et al., 2016; Yu et al., 2016). Although these HHOCs are less bioavailable compared with PCBs and low-brominated BDEs (Klosterhaus et al., 2011; Zhang et al., 2013), they have been detected in aquatic organisms (Zhang et al., 2013; Sun et al., 2016), calling for monitoring their occurrence in the environment.

Passive sampling provides a cost-effective way to monitor hydrophobic organic contaminants (HOCs) in the environment, showing a potential for developing global aquatic monitoring networks (Lohmann et al., 2017). Polydimethylsiloxane (PDMS) has been successfully used as passive samplers to measure the freely dissolved concentration ( $C_{free}$ ) of HOCs with moderate hydrophobicity, e.g. polycyclic aromatic hydrocarbons (PAHs) and PCBs (Rusina et al., 2007; Mayer et al., 2014). Nevertheless, its application for HHOCs remains challenging for the high uncertainty of PDMS-water partition coefficients ( $K_{PDMS,W}$ ) (Booij et al., 2015). It becomes increasingly challenging to accurately quantify  $C_{free}$  with increasing HOCs' hydrophobicity which results in extremely low  $C_{free}$ . Recently, Jahnke et al. (2012, 2014a) directly estimated thermodynamic bioaccumulation potential of sediment-bound HOCs through PDMS concentrations at equilibrium and lipid-PDMS partition coefficients ( $K_{lip,PDMS}$ ), offering a means to estimate bioaccumulation using passive samplers without the necessity of measuring  $C_{free}$ . Compared with  $K_{PDMS,W}$ , measuring  $K_{lip,PDMS}$  is more approachable and accurate (Jahnke et al., 2012), because lipid and PDMS have similar sorption capacities for HOCs.

When assessing the bioaccumulation potential of HOCs, lipids are regarded as the main accumulation phase in organism and HOC concentrations are normalized to a unified lipid, which is defined operationally based on experimental approaches and commonly contains both storage lipid (SL) and membrane lipid (ML). In fact, SL and ML are significantly different in structure and affinity for HOCs (Endo et al., 2011; Quinn et al., 2014) and the binding of chemicals to ML may cause adverse effects to organisms (Escher and Schwarzenbach, 2002). Besides lipid, other biological phases, e.g. protein, also involve in chemical sorption and form an important sorptive phase, particularly in lean organisms which contain high protein contents, such as benthic invertebrates (de Bruyn and Gobas, 2007; Elissen et al., 2010). Therefore, it is good to include SL, ML and protein as individual biocomponents and measure their respective partition coefficients to PDMS ( $K_{SL,PDMS}$ ,  $K_{ML,PDMS}$  and  $K_{pro,PDMS}$ ) when estimating HOC bioaccumulation using PDMS-based methods.

The main aim of the present study was to measure the values of  $K_{SL,PDMS}$ ,  $K_{ML,PDMS}$  and  $K_{pro,PDMS}$  for a variety of HOCs, including PCBs, PBDEs and HHOCs. To determine partition coefficients, both uptake methods (chemicals uptake from spiked biological phases to PDMS until equilibrium, e.g. Jahnke et al., 2008, Li et al., 2014 and Mäenpää et al., 2015a) and depletion methods (chemicals being released from spiked PDMS to biological phases until equilibrium, e.g. Escher et al., 2011 and Endo et al., 2013) have been applied. For some PCBs and low-brominated BDEs which have moderate hydrophobicity, both methods worked equally in measuring their partition coefficients

(Jahnke et al., 2008; Endo et al., 2013; Li et al., 2014; Mäenpää et al., 2015a), but no data are available for HHOCs between lipid and PDMS. Endo et al. (2013) tried to quantify  $K_{ML,PDMS}$  and  $K_{pro,PDMS}$  for PBDEs using the depletion method, but failed for chemicals more hydrophobic than BDE-183. Before depletion, HOCs were required to be loaded onto PDMS, which was usually achieved by soaking PDMS in methanol/water solution containing HOCs. This loading technique, however, was not applicable for HHOCs as suggested by the high disk-to-disk variability of BDE-209 in PDMS (>40%) (Endo et al., 2013). Alternatively, Li et al. (2014) used an uptake method for estimating PBDEs'  $K_{pro,PDMS}$ . Although both studies (Endo et al., 2013; Li et al., 2014) obtained similar  $K_{pro,PDMS}$  values for low-brominated BDEs, the values for BDE-183 were quite disparate. Therefore, it is necessary to develop additional methods to determine  $K_{lip,PDMS}$  ( $K_{SL,PDMS}$  and  $K_{ML,PDMS}$ ) and  $K_{pro,PDMS}$  values for HHOCs and interpret the deviation of  $K_{pro,PDMS}$  values for BDE-183 between the studies (Endo et al., 2013; Li et al., 2014).

To achieve this, a depletion method with preloaded PDMS disks was developed to determine  $K_{SL,PDMS}$ ,  $K_{ML,PDMS}$  and  $K_{pro,PDMS}$  for HOCs with a broad range of hydrophobicity (logarithm of octanol-water partition coefficients ( $\log K_{OW}$ ) from 5.07 to 11.6, HHOCs included). Furthermore, the impacts of HOC hydrophobicity and PDMS thickness on the partitioning process were assessed. The divergent data among studies (Endo et al., 2013, Li et al., 2014 and the present study) were explained. Lastly, the application of  $K_{SL,PDMS}$ ,  $K_{ML,PDMS}$  and  $K_{pro,PDMS}$  in estimating bioaccumulation potential of HOCs was discussed.

## 2. Materials and methods

### 2.1. Surrogates for lipids and proteins

Commercial corn oil, egg phosphatidylcholine (PC) and bovine serum albumin (BSA) were selected as the surrogates for SL, ML and protein, respectively. Geisler et al. (2012) found different SLs showed similar affinity for HOCs, which was further validated by the fact that there was no difference among the  $K_{SL,PDMS}$  values for PCBs when vegetable oil, fish oil or seal oil was used as the surrogate for SL (Jahnke et al., 2008). The PC is the main component of biological membranes and serum albumin is the most abundant protein in the serum, thus they were previously selected as the surrogates for ML and protein, respectively (Endo and Goss, 2011; Escher et al., 2011; Endo et al., 2013; Mäenpää et al., 2015a).

Corn oil (Arawana Brand, Shanghai, China) was bought in a local supermarket and egg PC (purity > 98%) and BSA were purchased from Shanghai Advanced Vehicle Technology Pharmaceutical Ltd. (Shanghai, China) and Boao biotech (Shanghai, China), respectively. Egg PC suspension (100 mg/mL) and BSA solutions (20, 60 and 100 mg/mL) were prepared in solution containing 0.9% NaCl and 8 mmol/L  $\text{NaN}_3$ . Before use, the egg PC suspension was vigorously stirred for 2 h to create liposomes (Mäenpää et al., 2015a).

### 2.2. Preparation of preloaded PDMS disks

The PDMS disks preloaded with HOCs were homemade from MDX4-4210 BioMedical Grade Elastomer kit which was purchased from Dow Corning (Auburn, MI, USA). According to the manufacturer's manual, elastomer component and curing agent (10:1, w/w) were thoroughly mixed. In the meantime, 2 mL of HOC solution in acetone was added to 23 g elastomer mix. To avoid oversaturation, HOC concentrations in PDMS were kept much lower than their solubility in PDMS (Grant et al., 2016). Then, the mixtures were coated on clean smooth

stainless steel plates using a film applicator (Fangzhou Coating Equipment Company, Guangzhou, China) to produce PDMS paste with nominal thicknesses of 100, 200 and 400  $\mu\text{m}$ .

After curing for 3 d at room temperature, PDMS films were peeled from the plates, cut into round pieces with a diameter of 22 mm and stored at 4 °C. Meanwhile, blank PDMS disks without HOCs were also prepared as above.

To ensure homogeneity of the PDMS disks, all disks were weighed. Eight pieces for each thickness were randomly sampled and the thickness was measured using microscope. The measured thickness of the three PDMS disks was 58, 108 and 209  $\mu\text{m}$  on average. Moreover, HOC concentrations in PDMS disks were analyzed in eight replicates for each thickness to evaluate the loading efficiency for all target chemicals.

### 2.3. Determination of $K_{\text{SL,PDMS}}$ , $K_{\text{ML,PDMS}}$ and $K_{\text{pro,PDMS}}$

Using the preloaded PDMS disks,  $K_{\text{SL,PDMS}}$ ,  $K_{\text{ML,PDMS}}$  and  $K_{\text{pro,PDMS}}$  were determined using the depletion method. The  $K_{\text{SL,PDMS}}$  and  $K_{\text{ML,PDMS}}$  were measured with 209- $\mu\text{m}$  PDMS disks, while  $K_{\text{pro,PDMS}}$  values were determined using the disks with three thicknesses (58, 108 and 209  $\mu\text{m}$ ). One preloaded PDMS disk was put into a 20-mL vial containing 0.4 g of corn oil, 1 mL of egg PC suspension (100 mg/mL) or 1 mL of BSA solution (20, 60 and 100 mg/mL for 58-, 108- and 209- $\mu\text{m}$  disk, respectively). The vials containing egg PC suspension and BSA solution were shaken at 200 rpm and all the treatments were kept at 23 °C in darkness.

At predetermined time intervals (Table S1, "S" represents figures and tables in the Supplementary data thereafter), the experiments were terminated in triplicate by retrieving PDMS disks from the vials using clean tweezers. For corn oil, PDMS disks were wiped clean, quickly dipped into acetone, then rinsed with deionized water, wiped dry and finally soaked in 5 mL of acetone for extraction. Alternatively, PDMS disks removed from egg PC suspension and BSA solution were directly rinsed with deionized water, wiped dry and soaked in 5 mL of acetone. After extraction, target HOCs were analyzed in all surrogate phases and the respective PDMS disks.

### 2.4. Chemical analysis

As shown in Table S2, target analytes included 21 PCBs, 14 PBDEs, *syn*-DP, *anti*-DP and DBDPE, covering wide ranges of hydrophobicity ( $\log K_{\text{OW}}$  of 5.07–11.6) and molecular weight (223–971 g/mol). The concentrations of target HOCs in the PDMS disks, corn oil, egg PC suspension and BSA solution were analyzed on an Agilent 7820 gas chromatograph/electron capture detector (GC/ECD) after solvent extraction, cleanup with multi-layer silica gel columns and concentrated sulfuric acid. In addition, GC/mass spectrometry was used to confirm GC/ECD quantification. More details on the target analytes, surrogates, internal standards and other reagents are provided in the Supplementary Data, as well as sample preparation and instrumental analysis methods.

To ensure the quality of analytical data, quality control samples were analyzed with test samples simultaneously. A calibration standard was analyzed every 10 samples on GC/ECD and the differences between the calibration check standards were within 20% for all analytes. A method blank (solvent), a matrix blank (blank PDMS disk or biological phases), a matrix spike and its duplicate (PDMS disk or biological phases spiked with target analytes) were included for every 20 samples. No target compound was detected in the blanks. Except for relatively high recovery of DBDPE in spiked corn oil (128%–135%), the recoveries of target compounds in all matrix spike samples were all in a range of 62.0% to 110% (Table S3). In addition, three surrogates (4,4'-dibromooctafluorobiphenyl (DBOFB), CB-67 and CB-169) were added to all samples before extraction to check the performance of sample preparation processes, and their recoveries (84.2%–105%) are also presented in Table S3. The reporting limits (RLs) were calculated by multiplying the lowest concentration of calibration standards by the final

extract volume and then dividing by the weight of the sample (PDMS, corn oil, egg PC or BSA). Accordingly, the RLs were 0.32–6.25 ng/g for BDE-206, –207, –208 and –209, 0.13–2.50 ng/g for other PBDEs, PCBs and DP, and 0.63–12.5 ng/g for DBDPE.

### 2.5. Data analysis

Target HOCs in egg PC suspension and BSA solution were assumed to be mainly associated with the egg PC and BSA molecules, since the distribution in aqueous phase was negligible for HOCs with  $\log K_{\text{OW}} > 5$  (Escher et al., 2011). Therefore, chemical concentrations in egg PC and BSA were calculated by dividing HOC mass by the masses of egg PC and BSA, respectively.

A first-order one-compartment kinetic model (Scientist, Micromath, Salt Lake City, USA) was fit to predict the kinetic rate constant  $k$  (Eq. (1)). Target HOCs in the preloaded PDMS disks desorbed into the biological phases, and the concentration of a HOC in the biological phase  $C_t$  increased with depletion time  $t$  until attaining its equilibrium concentration  $C$ . The time to reach apparent equilibrium ( $t_{95}$ ) was also calculated (Eq. (2)).

$$C_t = C \times (1 - e^{-kt}) \quad (1)$$

$$t_{95} = \frac{-\ln(0.05)}{k} \quad (2)$$

Then,  $K_{\text{SL,PDMS}}$ ,  $K_{\text{ML,PDMS}}$  and  $K_{\text{pro,PDMS}}$  were determined by dividing HOC concentration in individual biological phases at equilibrium ( $C_{\text{oil}}$ ,  $C_{\text{PC}}$  or  $C_{\text{BSA}}$ ) by its concentration in PDMS ( $C_{\text{PDMS}}$ ) (Eqs. (3)–(5)). Relative sorption capacity (RSC%) of individual biological phases were calculated using Eqs. (6)–(8) (Mäenpää et al., 2015a).

$$K_{\text{SL,PDMS}} (\text{g}_{\text{PDMS}} \cdot \text{g}_{\text{oil}}^{-1}) = \frac{C_{\text{oil}} (\text{ng} \cdot \text{g}_{\text{oil}}^{-1})}{C_{\text{PDMS}} (\text{ng} \cdot \text{g}_{\text{PDMS}}^{-1})} \quad (3)$$

$$K_{\text{ML,PDMS}} (\text{g}_{\text{PDMS}} \cdot \text{g}_{\text{PC}}^{-1}) = \frac{C_{\text{PC}} (\text{ng} \cdot \text{g}_{\text{PC}}^{-1})}{C_{\text{PDMS}} (\text{ng} \cdot \text{g}_{\text{PDMS}}^{-1})} \quad (4)$$

$$K_{\text{pro,PDMS}} (\text{g}_{\text{PDMS}} \cdot \text{g}_{\text{BSA}}^{-1}) = \frac{C_{\text{BSA}} (\text{ng} \cdot \text{g}_{\text{BSA}}^{-1})}{C_{\text{PDMS}} (\text{ng} \cdot \text{g}_{\text{PDMS}}^{-1})} \quad (5)$$

$$\text{RSC}_{\text{SL}}\% = \frac{K_{\text{SL,PDMS}}}{K_{\text{SL,PDMS}} + K_{\text{ML,PDMS}} + K_{\text{pro,PDMS}}} \times 100 \quad (6)$$

$$\text{RSC}_{\text{ML}}\% = \frac{K_{\text{ML,PDMS}}}{K_{\text{SL,PDMS}} + K_{\text{ML,PDMS}} + K_{\text{pro,PDMS}}} \times 100 \quad (7)$$

$$\text{RSC}_{\text{pro}}\% = \frac{K_{\text{pro,PDMS}}}{K_{\text{SL,PDMS}} + K_{\text{ML,PDMS}} + K_{\text{pro,PDMS}}} \times 100 \quad (8)$$

## 3. Results and discussion

### 3.1. Loading efficiency of HOCs to PDMS disks

The PDMS disks were prepared in three thicknesses and disk-to-disk variations of the disks' weight were small, with the relative standard deviations (RSD) of 9.3%, 8.1% and 3.2% for disks with thickness of 58 ( $n = 59$ ), 108 ( $n = 33$ ) and 209  $\mu\text{m}$  ( $n = 84$ ), respectively. This indicated the PDMS disks were uniformly formed. The target HOCs were also homogeneously distributed in the preloaded PDMS disks as indicated by the small disk-to-disk variability of  $C_{\text{PDMS}}$  (eight replicates for each thickness) for all chemicals including HHOCs. As shown in Table S4, the RSDs were <20% for all HOCs (<10% for most HOCs) except CB-8 in 58- $\mu\text{m}$  disk (43%) due to its high volatility. Compared with over 40%

of loading variability for BDE-209 in post-loaded PDMS disk by Endo et al. (2013), the variability for  $C_{\text{PDMS}}$  of BDE-209 across disks in the current study was exceptionally lower (1.0%–5.8%). Thus, the newly developed method by mixing HOC solution into the PDMS elastomer kit before polymerization overcame the challenge of loading HHOCs to PDMS disks using the traditional methanol/water post-loading method (Brown et al., 2001).

Loading efficiency of individual HOCs in preloaded PDMS disks were calculated as the ratio of measured and nominal  $C_{\text{PDMS}}$  and ranged from 8.34% (CB-8) to 113% (anti-DP), which were positively related to the boiling points of HOCs (Table S4). As shown in Table S4, measured  $C_{\text{PDMS}}$  of highly chlorinated PCBs, PBDEs and DPs nearly approached their nominal concentrations, which validated the effectiveness of this loading method for HHOCs. Loading efficiency of DBDPE was lower than other HHOCs although it also has low volatility. This may be a result of relatively low solubility of DBDPE in most solvents.

In addition to volatility, loading efficiency was also influenced by the thickness of PDMS disks. In general, the thicker the disk, the higher the loading efficiency. Chemicals with lower boiling points tend to volatilize during the curing process and thinner polymers facilitated the volatilization. With almost 100% loading efficiency for HHOCs, low loading variation and customizable thickness of PDMS disks, the proposed method provided a viable means to load HHOCs to PDMS for further studying their partitioning behaviors or serving as performance reference compounds for passive sampling.

### 3.2. Depletion kinetics of HOCs from preloaded PDMS disk to biological phases

The depletion testing was initiated by introducing the preloaded PDMS disks into biological phases (oil, egg PC or BSA solution). The total mass of individual HOCs in the whole partitioning system was expected to be the same before and after depletion. Except for DBDPE in corn oil (66.7%), the sum mass of individual HOCs in the whole partitioning system equaled 74.1%–121% ( $99.5\% \pm 15.4\%$ ) of the chemical mass in the preloaded PDMS before depletion (Fig. S1). This mass balance ensured the validity of the experiments.

In the preloading method, un-reacted silicone residues could not be removed from the cured PDMS disks by organic solvent extraction and may influence the partition coefficients. To evaluate the impact, additional PDMS disks for each thickness were prepared and extracted with acetone. The amount of un-reacted residues in cured PDMS was estimated as the loss of PDMS weight before and after acetone extraction. The average weight changed from 25.8 to 25.4 mg, 47.9 to 46.2 mg and 92.9 to 88.7 mg for 58-, 108-, and 209- $\mu\text{m}$  PDMS disks, respectively, suggesting that only small portion of silicone residues (1.55%, 3.54% and 4.52%, respectively) were not crosslinked. Therefore, the influence of the un-reacted silicone residues on the partition coefficients was not corrected in the current study.

The sorption of lipid into PDMS may also cause erroneous estimation of  $C_{\text{PDMS}}$  (Jahnke et al., 2008; Jin et al., 2013). To evaluate PDMS fouling by corn oil, six blank 209- $\mu\text{m}$  PDMS disks (a mean of 92.9 mg) were accurately weighed before and after soaking the disks in corn oil for 24 h. The change of PDMS weight could not be quantified on the balance with a minimum range of 0.1 mg. Suppose that the maximum of 0.1 mg oil partitioned into a PDMS disk and  $K_{\text{SL,PDMS}}$  of HOCs ranged from 14.5 to 62.9 g/g (Jahnke et al., 2008), the mass of HOCs in corn oil which was sorbed into PDMS only accounted for 1.5%–6.3% of total HOCs in PDMS. This suggested that the influence of lipid on  $C_{\text{PDMS}}$  was negligible and thus  $C_{\text{PDMS}}$  was not corrected in oil depletion testing.

To ensure the equilibrium was reached between PDMS and biological phases, series samplings were conducted and data were fit to a first-order one-compartment model (Eq. (1)). Fig. 1 showed depletion kinetic curves of CB-44, CB-180 and BDE-196 ( $\log K_{\text{OW}}$  5.75, 7.36 and 9.29, respectively) in corn oil, egg PC suspension and BSA and the three compounds were the representative HOCs with moderate, high and

extremely high hydrophobicity. Kinetic curves of other chemicals are plotted in Figs. S2–S6.

Kinetic rate constants ( $k$ ) and the time to reach equilibrium ( $t_{95}$ ) were estimated using Eqs. (1) and (2) (Table S2). Generally, desorption of HOCs from PDMS to biological phases was the fastest for corn oil, followed by BSA solution, and egg PC suspension was the slowest. Regardless of their hydrophobicity, apparent equilibrium was achieved between corn oil and PDMS within 0.1–0.3 h for all HOCs under static conditions except for DBDPE whose  $t_{95}$  was 7.62 h under orbital shaking at 200 rpm. Slower desorption of DBDPE from PDMS to oil may be related to its higher molecular weight than other chemicals.

Compared with corn oil, it took more time to reach equilibrium between PDMS and egg PC/BSA. The  $t_{95}$  prolonged with increasing  $\log K_{\text{OW}}$  until 8 and kept almost stable for HHOCs. The  $t_{95}$  of HOCs in egg PC-PDMS system increased from 8.51 h (CB-8) to 250 h (CB-87), while  $t_{95}$  in BSA-PDMS (209  $\mu\text{m}$ ) were relatively shorter with values between 0.55 h (CB-8) and 254 h (CB-209). As shown in Fig. S4,  $C_{\text{BSA}}$  of BDE-209 from 209- $\mu\text{m}$  PDMS continued increasing and could not reach equilibrium until the end of depletion experiment. When thinner PDMS disks were used, the equilibrium of BDE-209 in BSA solution was attained (Fig. S5–S6). Conversely,  $C_{\text{BSA}}$  of DP and DBDPE showed nearly no change throughout the depletion process in BSA-PDMS system regardless of PDMS thickness (Fig. S4–S6), indicating unexpectedly fast equilibrium. “Pseudo-equilibrium” has been previously reported for uptake of HOCs into PDMS-coated fibers (Brennan et al., 2009), and Xie et al. (2009) demonstrated that if uptake time was long enough,  $C_{\text{PDMS}}$  would reach a new equilibrium after the “pseudo-equilibrium”. This “pseudo-equilibrium” may be the reason for the observed fast equilibrium between the preloaded PDMS and BSA solution for DP and DBDPE. In this case, the depletion only occurred on the edge of PDMS disks, resulting in relatively high variance of  $C_{\text{BSA}}$  of DP and DBDPE.

### 3.3. Determination of $K_{\text{SL,PDMS}}$ , $K_{\text{ML,PDMS}}$ and $K_{\text{pro,PDMS}}$

The partition coefficients of HOCs between biological phases and PDMS were determined at equilibrium using Eqs. (3)–(5) (Table 1). Since  $C_{\text{BSA}}$  of BDE-208 and its  $C_{\text{PDMS}}$  after oil depletion were below the RLs, no  $K_{\text{SL,PDMS}}$  and  $K_{\text{pro,PDMS}}$  of BDE-208 were estimated. The  $K_{\text{SL,PDMS}}$  values fell within a narrow range despite the high variance of  $K_{\text{OW}}$  values (>6 orders of magnitude) and molecular weight of target HOCs. As plotted in Fig. 2,  $K_{\text{SL,PDMS}}$  values for all HOCs ranged from 5.36 to 52.5 g/g (mean 23.9 g/g), which was in accordance with the previously reported  $K_{\text{SL,PDMS}}$  values for PCBs and organochlorine pesticides (14.5–62.9 g/g, Jahnke et al., 2008), low-brominated BDEs (4.6–53.5 g/g, Allan et al., 2013) and polychlorinated dibenzo-*p*-dioxins (20–38 g/g, Jin et al., 2013), although the HHOCs in the present study have much higher hydrophobicity.

Partition capability of HOCs in PC reflected their affinity for the membranes which was partly associated with the toxicity (Endo et al., 2011). Comparatively,  $K_{\text{ML,PDMS}}$  were lower than  $K_{\text{SL,PDMS}}$  with values between 0.286 and 11.8 g/g (mean  $\pm$  SD:  $3.96 \pm 3.23$  g/g) (Fig. 2), indicating smaller affinity of HOCs for ML than SL. This was in line with previous results that partition coefficients of chemicals between SL and water ( $K_{\text{SL,W}}$ ) were generally higher than those between ML and water ( $K_{\text{ML,W}}$ ) (Endo et al., 2011; Quinn et al., 2014). Quinn et al. (2014) calculated partition coefficients between SL and ML ( $K_{\text{SL,ML}}$ ) by dividing  $K_{\text{SL,W}}$  by  $K_{\text{ML,W}}$  for 18 PCBs and the  $K_{\text{SL,ML}}$  were 2.95 g/g on average. Endo et al. (2011) reported that  $K_{\text{SL,ML}}$  values were <10 g/g for HOCs with  $\log K_{\text{OW}} < 7$ . Similarly,  $K_{\text{SL,ML}}$  values were computed by dividing  $K_{\text{SL,PDMS}}$  by  $K_{\text{ML,PDMS}}$  in the present study and  $K_{\text{SL,ML}}$  ranged from 2.86–5.74 g/g for HOCs with  $\log K_{\text{OW}} < 7$  (Fig. S7), which was in good agreement with previous studies.

Mäenpää et al. (2015a) have previously measured  $K_{\text{ML,PDMS}}$  values for CB-77 and -153 (3.0 and 2.2 g/g, respectively) and they were lower than the values in the present study (11.5 and 4.99 g/g, respectively). Endo et al. (2013) have estimated  $K_{\text{ML,PDMS}}$  values for BDE-28, -47, -99, -100, -153,

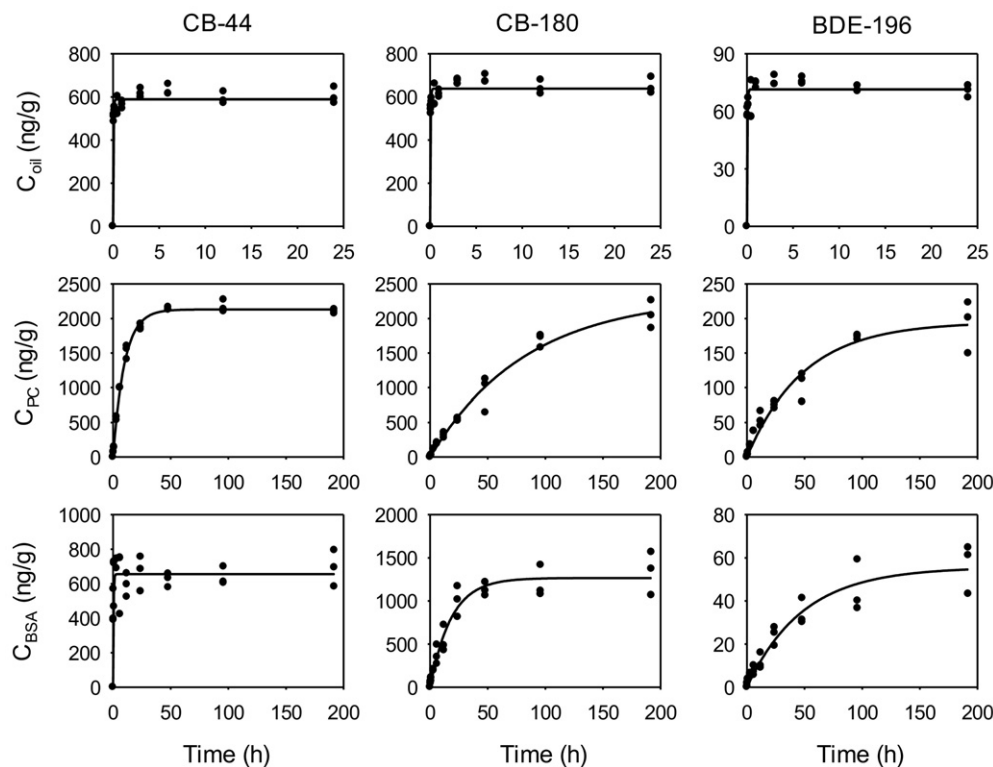


**Fig. 1.** Kinetic curves of polychlorinated biphenyl (CB)-44, CB-180 and polybrominated diphenyl ether (BDE)-196 in corn oil, 100 mg/mL egg phosphatidylcholine (PC) suspension and 100 mg/mL bovine serum albumin (BSA) solution. The preloaded PDMS disks used in these partition systems had identical thickness (209  $\mu\text{m}$ ).

-154 and -183 (6.96 to 16.7 g/g) which were slightly higher than the current values. Different methods to prepare liposomes might be one of the reasons for differing  $K_{\text{ML,PDMS}}$  values. Standard filter extrusion method used by Endo et al. (2013) could gain the liposomes with uniform size, but the stirring method might not obtain the ideal liposomes and introduced some errors in estimating  $K_{\text{ML,PDMS}}$ . In addition, different types of PC and manufactures of PDMS might also influence the partition coefficients (Rusina et al., 2007; Endo et al., 2013).

Different from a uniformed  $K_{\text{SL,PDMS}}$  value across chemicals, variation in  $K_{\text{ML,PDMS}}$  was greater. Most  $K_{\text{ML,PDMS}}$  for HOCs with  $\log K_{\text{OW}} < 7$  were in a range of 3.60–11.8 g/g, but the values decreased for more hydrophobic HOCs. As  $\log K_{\text{ML,W}}$  and  $\log K_{\text{PDMS,W}}$  exhibited linear relationship against  $\log K_{\text{OW}}$  for HOCs with  $\log K_{\text{OW}} < 7$  (Muijs and Jonker, 2009; Di Filippo and Eganhouse, 2010; Endo et al., 2011), the partitioning between ML and PDMS was expected to be independent of hydrophobicity, which was supported by the similar  $K_{\text{ML,PDMS}}$  values for moderately hydrophobic compounds in the present study. For more hydrophobic contaminants, similar  $K_{\text{ML,PDMS}}$  values were also expected. However, measured  $K_{\text{ML,PDMS}}$  values started to decrease as  $\log K_{\text{OW}}$  exceeded 7, probably because the diffusion of the HHOCs in PDMS was limited but not in ML. This is in accordance with the curvilinear relationship between  $K_{\text{PDMS,W}}$  and  $K_{\text{OW}}$  (Yang et al., 2007). Interestingly, planar PCBs like CB-77, -105, -118 and -126 had significantly greater  $K_{\text{ML,PDMS}}$  values of 11.5, 8.30, 7.20 and 11.8 g/g, respectively, than other PCBs ( $3.50 \pm 1.96$  g/g). This demonstrated the impact of steric interactions of HOCs with the PDMS polymer network on the partitioning process (Yang et al., 2007; You et al., 2007).

Furthermore,  $K_{\text{pro,PDMS}}$  values of the HOCs ranged from 0.067 to 2.62 g/g with a mean value of 0.605 g/g (Table 1). As discussed above, DP and DBDPE were probably at “pseudo-equilibrium” between BSA and PDMS, thus they were excluded from the calculations. Although the affinity of HOCs for protein was approximately 40 and 6.5 times lower than SL and ML on average, respectively, protein can serve as an additional sorptive phase in lean organisms which have high protein contents (de Bruyn and Gobas, 2007).

Overall, with additional data of HHOCs, our study validated the hypothesis by Jahnke et al. (2016) that partition coefficients between SL and PDMS are largely independent of chemical hydrophobicity, promoting direct use of HOC concentrations in passive samplers for estimating their bioaccumulation potential with average  $K_{\text{SL,PDMS}}$  value of 23.9 g/g. Moreover, the ML and protein had a weaker affinity for HOCs than SL, and  $K_{\text{ML,PDMS}}$  (0.286–11.8 g/g) and  $K_{\text{pro,PDMS}}$  (0.067–2.62 g/g) were also less dependent of hydrophobicity than their partition coefficients from water.

### 3.4. Interpretation of divergent $K_{\text{PDMS,pro}}$

To compare  $K_{\text{pro,PDMS}}$  values obtained in the current study with previous studies,  $K_{\text{PDMS,pro}}$  which equals to  $1/K_{\text{pro,PDMS}}$  were used. The  $K_{\text{PDMS,pro}}$  values determined by 209- $\mu\text{m}$  PDMS were from 0.444 to 20.7 g/g (mean 6.17 g/g), excluding DP and DBDPE. The  $K_{\text{PDMS,pro}}$  values for PBDEs were also previously measured (Endo et al., 2013; Li et al., 2014), however, divergence was noted for HHOCs with  $\log K_{\text{OW}} > 8$  (Fig. 3). Endo et al. (2013) and the current study estimated  $K_{\text{PDMS,pro}}$  by the depletion of HOCs from the loaded PDMS to clean BSA solution, while Li et al. (2014) used an uptake method by exposing clean PDMS disks (200- $\mu\text{m}$  thickness) in 10 mg/mL BSA solution containing target compounds. Due to the challenge of loading BDE-209 to PDMS disks, the most hydrophobic compound reported by Endo et al. (2013) was BDE-183. Instead, Li et al. (2014) and the current study estimated  $K_{\text{PDMS,pro}}$  values for HHOCs. As shown in Fig. 3,  $K_{\text{PDMS,pro}}$  values were similar for PBDEs with  $\log K_{\text{OW}} < 8$  in the three studies, however, for the HHOCs with  $\log K_{\text{OW}} > 8$ ,  $K_{\text{PDMS,pro}}$  values estimated by the uptake method (Li et al., 2014) were considerably lower than those by the depletion methods (Endo et al., 2013 and the present study). The difference between the methods enlarged with increasing hydrophobicity and were up to three orders of magnitude for DBDPE. Thus, it is imperative to understand the divergence among the studies and obtain more accurate estimation of  $K_{\text{PDMS,pro}}$  for HHOCs.

**Table 1**  
Equilibrium partition coefficients between storage lipid, membrane lipid, protein and polydimethylsiloxane ( $K_{SL,PDMS}$ ,  $K_{ML,PDMS}$  and  $K_{pro,PDMS}$ , mean  $\pm$  standard deviation) at 23 °C.

Compound	$K_{SL,PDMS}$	$K_{ML,PDMS}$	$K_{pro,PDMS}^a$
CB-8	13.9 $\pm$ 1.4	4.87 $\pm$ 0.22	0.255 $\pm$ 0.049
CB-18	13.8 $\pm$ 1.5	3.60 $\pm$ 0.17	0.378 $\pm$ 0.057
CB-28	19.9 $\pm$ 2.0	4.95 $\pm$ 0.26	0.147 $\pm$ 0.017
CB-44	16.9 $\pm$ 2.0	4.32 $\pm$ 0.18	0.501 $\pm$ 0.045
CB-52	18.3 $\pm$ 2.1	3.83 $\pm$ 0.17	0.474 $\pm$ 0.044
CB-66	22.9 $\pm$ 2.5	6.17 $\pm$ 0.46	0.167 $\pm$ 0.026
CB-77	32.8 $\pm$ 3.6	11.5 $\pm$ 0.8	0.182 $\pm$ 0.016
CB-101	20.5 $\pm$ 2.5	4.70 $\pm$ 0.22	1.37 $\pm$ 0.17
CB-105	24.2 $\pm$ 2.6	8.30 $\pm$ 0.34	0.189 $\pm$ 0.014
CB-118	29.5 $\pm$ 3.4	7.20 $\pm$ 0.33	0.880 $\pm$ 0.098
CB-126	28.5 $\pm$ 3.0	11.8 $\pm$ 0.5	0.214 $\pm$ 0.023
CB-128	24.7 $\pm$ 3.0	6.63 $\pm$ 0.50	0.129 $\pm$ 0.010
CB-138	26.6 $\pm$ 3.4	5.54 $\pm$ 0.48	0.547 $\pm$ 0.055
CB-153	28.6 $\pm$ 3.8	4.99 $\pm$ 0.50	1.53 $\pm$ 0.18
CB-170	26.6 $\pm$ 3.4	3.44 $\pm$ 1.09	0.194 $\pm$ 0.019
CB-180	28.6 $\pm$ 3.6	2.99 $\pm$ 0.97	1.52 $\pm$ 0.25
CB-187	22.9 $\pm$ 3.1	2.55 $\pm$ 0.68	0.216 $\pm$ 0.021
CB-195	23.0 $\pm$ 2.9	1.16 $\pm$ 0.55	0.164 $\pm$ 0.020
CB-201	16.3 $\pm$ 2.2	0.795 $\pm$ 0.359	0.104 $\pm$ 0.011
CB-206	25.4 $\pm$ 3.3	0.663 $\pm$ 0.407	0.277 $\pm$ 0.034
CB-209	17.7 $\pm$ 2.4	0.350 $\pm$ 0.245	0.067 $\pm$ 0.010
BDE-47	33.0 $\pm$ 3.8	7.85 $\pm$ 0.35	0.872 $\pm$ 0.083
BDE-85	34.9 $\pm$ 6.1	11.1 $\pm$ 4.3	0.520 $\pm$ 0.050
BDE-99	35.4 $\pm$ 3.7	7.20 $\pm$ 0.13	1.48 $\pm$ 0.21
BDE-100	25.8 $\pm$ 2.8	4.94 $\pm$ 0.54	1.05 $\pm$ 0.13
BDE-153	27.7 $\pm$ 2.8	4.18 $\pm$ 1.10	2.13 $\pm$ 0.29
BDE-154	19.8 $\pm$ 2.7	3.14 $\pm$ 1.02	0.772 $\pm$ 0.108
BDE-183	39.8 $\pm$ 5.6	2.33 $\pm$ 1.09	2.63 $\pm$ 0.87
BDE-196	30.4 $\pm$ 4.6	1.75 $\pm$ 1.03	0.380 $\pm$ 0.014
BDE-197	52.5 $\pm$ 7.1	1.11 $\pm$ 0.56	0.185 $\pm$ 0.002
BDE-203	5.36 $\pm$ 0.44	0.981 $\pm$ 0.447	0.561 $\pm$ 0.010
BDE-206	7.39 $\pm$ 0.38	1.04 $\pm$ 0.45	0.209 $\pm$ 0.057
BDE-207	16.8 $\pm$ 1.2	0.936 $\pm$ 0.493	0.146 $\pm$ 0.009
BDE-208	na <sup>b</sup>	0.306 $\pm$ 0.097	na
BDE-209	25.5 $\pm$ 1.8	2.15 $\pm$ 1.17	0.154 $\pm$ 0.017
syn-DP	14.4 $\pm$ 2.2	0.286 $\pm$ 0.178	0.00430 $\pm$ 0.00100 <sup>c</sup>
anti-DP	23.5 $\pm$ 2.2	0.333 $\pm$ 0.205	0.00325 $\pm$ 0.00098 <sup>c</sup>
DBDPE	10.1 $\pm$ 2.2	0.519 $\pm$ 0.190	0.0480 $\pm$ 0.0287 <sup>c</sup>

<sup>a</sup> The  $K_{pro,PDMS}$  values were determined using 58- $\mu$ m preloaded PDMS disks.

<sup>b</sup> Not available.

<sup>c</sup> The values were likely underestimated by "pseudo-equilibrium".

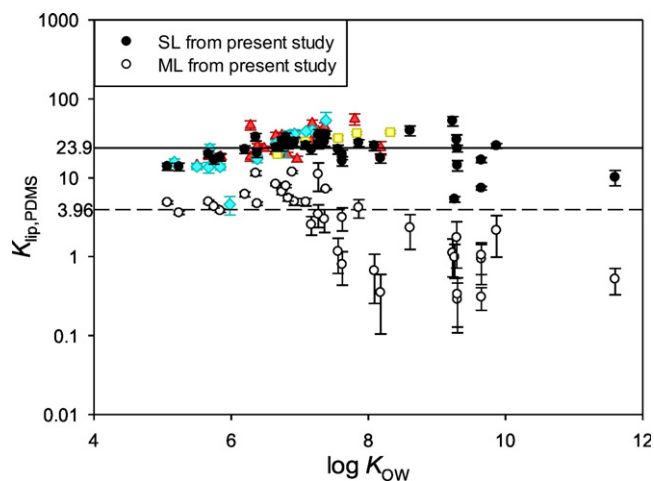


**Fig. 2.** Lipid (lip)-polydimethylsiloxane (PDMS) partition coefficients ( $K_{lip,PDMS}$ , including storage lipid (SL)-PDMS partition coefficients ( $K_{SL,PDMS}$ ) and membrane lipid (ML)-PDMS partition coefficients ( $K_{ML,PDMS}$ )) against logarithm of octanol-water partition coefficients ( $\log K_{OW}$ ). The solid and dotted lines stand for the average values of  $K_{SL,PDMS}$  and  $K_{ML,PDMS}$  obtained in the present study, respectively. The red triangles were SL data from Jahnke et al., 2008, blue rhombuses from Allan et al., 2013, and yellow squares from Jin et al., 2013.

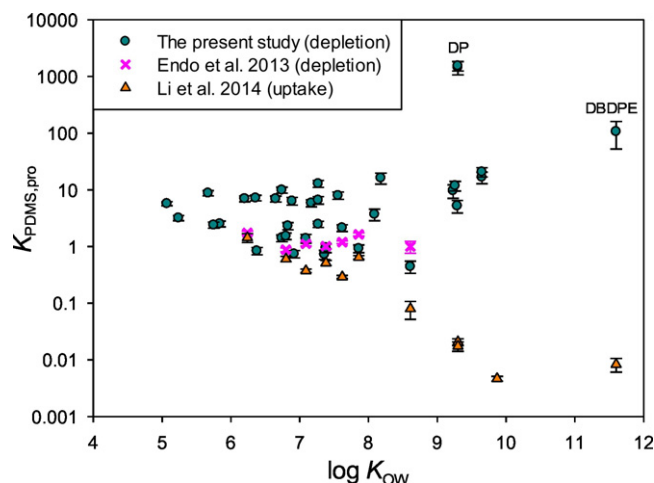


**Fig. 3.** Comparison of polydimethylsiloxane (PDMS)-protein partition coefficients ( $K_{PDMS,pro}$ ) for hydrophobic organic compounds among studies (Endo et al., 2013, Li et al., 2014, the measurements of 209- $\mu$ m preloaded PDMS disks in the present study). The  $K_{PDMS,pro}$  values are shown against logarithm of octanol-water partition coefficients ( $\log K_{OW}$ ). Note that the values for dechlorane plus (DP) and decabromodiphenyl ethane (DBDPE) might be significantly biased by "pseudo-equilibrium".

As shown in Fig. S4, BDE-209 did not reach equilibrium between 209- $\mu$ m PDMS and BSA solution until the termination of depletion testing and DP and DBDPE were in "pseudo-equilibrium", indicating slow diffusion of HHOCs in PDMS polymer. This likely explained the divergent  $K_{PDMS,pro}$  values between the depletion and uptake methods. Diffusion coefficients of PCBs and PBDEs in PDMS decreased with increasing molecular weight (Rusina et al., 2010; Valderrama et al., 2016). The HHOCs have large molecular size, which hindered their diffusion in PDMS (Yang et al., 2007). As a consequence, "pseudo-equilibrium" only occurred for HHOCs on the edge of PDMS and BSA solution. On the contrary, HHOCs in the polymer center contribute little to the equilibrium. In depletion method, the HHOCs on the edge of the preloaded PDMS disks quickly reached "pseudo-equilibrium" with BSA solution, subsequently a concentration gradient of HHOCs from the center ( $C_{PDMS,inner}$ ) to the edge of the PDMS disk ( $C_{PDMS,edge}$ ) after a certain time of depletion (Fig. 4A). Nevertheless, measured  $C_{PDMS}$  before depletion was used for calculating  $K_{PDMS,pro}$  instead of  $C_{PDMS,edge}$ , which were truly in "pseudo-equilibrium" with  $C_{BSA}$ . As a result,  $K_{PDMS,pro}$  values of HHOCs in the present study were overestimated. By contrast, in the uptake method, HHOCs in spiked BSA solution quickly partitioned to the edge of PDMS disks but hardly diffused into inner PDMS (Yang et al., 2007), causing  $C_{PDMS,edge}$  being higher than  $C_{PDMS}$ . The use of  $C_{PDMS}$  for the calculation underestimated  $K_{PDMS,pro}$  values for HHOCs. Hence,  $K_{PDMS,pro}$  values derived from the uptake method were much lower than those from the depletion method, and the discrepancy enlarged when molecular size of HHOCs increased (Fig. 3).

To verify the assumption, preloaded PDMS disks were prepared in three thicknesses and used to measure HHOCs'  $K_{PDMS,pro}$  values. In theory, as depicted in Fig. 4A, the difference between  $C_{PDMS,inner}$  and  $C_{PDMS,edge}$  would be smaller and subsequently the estimation of  $K_{PDMS,pro}$  would be more accurate when using thinner PDMS. In depletion method, smaller  $K_{PDMS,pro}$  values would be noted for thinner PDMS disks. Fig. 4B showed  $K_{PDMS,pro}$  values estimated using 58-, 108- and 209- $\mu$ m PDMS. When HOCs had  $\log K_{OW} < 9$ ,  $K_{PDMS,pro}$  values were similar regardless of PDMS thickness. As we expected, however,  $K_{PDMS,pro}$  values of HHOCs significantly reduced when thinner disks were used. For example,  $K_{PDMS,pro}$  of BDE-207 dropped from  $16.7 \pm 3.8$  (209- $\mu$ m PDMS) to  $13.7 \pm 1.1$  (108- $\mu$ m) and to  $6.85 \pm 0.41$  g/g (58- $\mu$ m).

Except for DP and DBDPE,  $K_{PDMS,pro}$  values calculated using 58- $\mu$ m PDMS were in the range of 0.382–14.9 g/g (mean 3.84 g/g), which

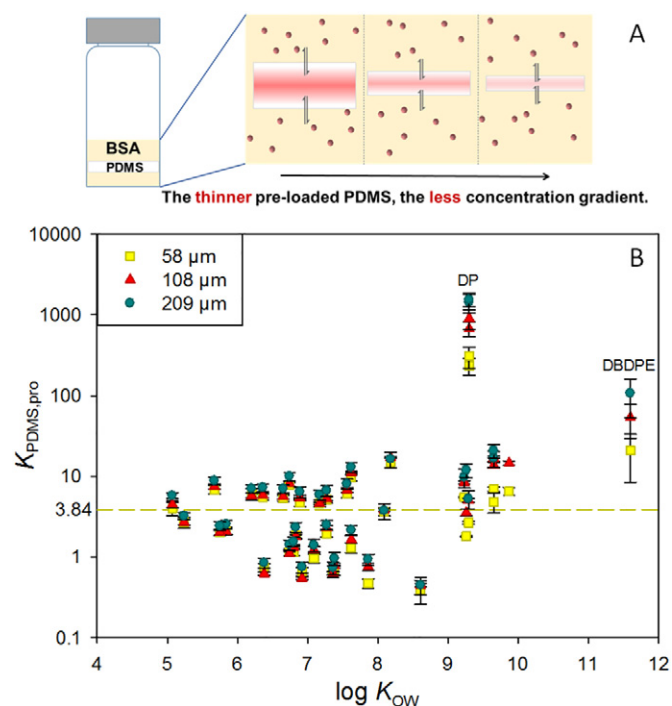


**Fig. 4.** The impact of "pseudo-equilibrium" causing by slow diffusion of chemicals in polydimethylsiloxane (PDMS) on the measurement of PDMS-protein partition coefficients ( $K_{\text{PDMS,pro}}$ ) with preloaded PDMS disks. (A) Theoretical diagram of "pseudo-equilibrium" between PDMS and protein; (B) The  $K_{\text{PDMS,pro}}$  measured with 58-, 108- and 209- $\mu\text{m}$  preloaded PDMS disks against logarithm of octanol-water partition coefficients ( $\log K_{\text{OW}}$ ). The dotted line stands for average  $K_{\text{PDMS,pro}}$  value measured using 58- $\mu\text{m}$  preloaded PDMS disks. Note that the values for dechlorane plus (DP) and decabromodiphenyl ethane (DBDPE) might be significantly biased by "pseudo-equilibrium".

were regarded to be the most accurate estimates the current study. To continue decreasing PDMS thickness and prolonging depletion time, the accuracy of  $K_{\text{PDMS,pro}}$  values for DP and DBDPE would be improved and possibly fall in the similar range as other HOCs. This confirmed that the partition coefficients of HOCs between PDMS and biological phases were independent of hydrophobicity and passive samplers were viable to predict bioaccumulation potential for HHOCs.

### 3.5. Application of partition coefficients between biological phases and PDMS

Accumulation capacity of SL, ML and protein in biota was compared by calculating relative sorption capacity (RSC) of individual biological components using Eqs. (6)–(8) (Fig. S8). The RSC followed the order of SL > ML > protein, and SL predominated partitioning capacity with RSC ranging from 70.3% to 98.6%. The ML played an important role in HOC bioaccumulation in tissues which were rich of ML, such as brain, kidney and liver (Mäenpää et al., 2015a). The RSC of protein were relatively small (<8%), yet the accumulation of HOCs in protein cannot be ignored, especially for invertebrates which usually have high contents of protein. For example, *Lumbricus variegatus* contains 11.1% of lipid and 62.2% of protein on a dry weight basis (van der Heijden et al., 2015). For this species, HOCs accumulated in protein may account for one-third of their total mass in organism because of high percentage of protein. Nevertheless, as BSA commonly showed higher sorption capacity than structural proteins, like muscle proteins, collagen and gelatin (Endo et al., 2012), possible overestimation of protein bioaccumulation by using BSA-derived  $K_{\text{pro,PDMS}}$  values should be noted.

Thermodynamic bioaccumulation potential of HOCs in environmental media could be directly estimated from equilibrium concentrations in PDMS-based passive samplers and  $K_{\text{SL,PDMS}}$ ,  $K_{\text{ML,PDMS}}$  and  $K_{\text{pro,PDMS}}$ .

Some researchers have used  $C_{\text{PDMS}}$  which was equilibrated with sediment and  $K_{\text{SL,PDMS}}$  to calculate equilibrium partition concentrations of HOCs in lipid ( $C_{\text{lipid,partition}}$ ) and compare with measured lipid-normalized concentrations in biota ( $C_{\text{lipid,biota}}$ ) which were quantified using exhaustive extraction. Mäenpää et al. (2011) reported  $C_{\text{lipid,partition}}$  of PCBs were two times higher than  $C_{\text{lipid,biota}}$  in *L. variegatus* exposed in lake sediment. Jahnke et al. (2012) also found that  $C_{\text{lipid,partition}}$  of PCBs were about five times higher than  $C_{\text{lipid,biota}}$  in fish from Baltic Sea. Moreover,  $C_{\text{lipid,partition}}$  of PCBs were higher than  $C_{\text{lipid,biota}}$  in mussels and fish (Jahnke et al., 2014b; Mäenpää et al., 2015b; Schäfer et al., 2015), but hexachlorobenzene was approaching equilibrium (Jahnke et al., 2014a). Overall,  $C_{\text{lipid,partition}}$  were generally higher than  $C_{\text{lipid,biota}}$ , implying accumulation of HOCs in most field-collected organisms didn't achieve equilibrium. In the previous estimation, the accumulation of HOCs in ML and protein was often neglected. If all biological phases were all taken into consideration, the prediction might be more accurate.

## 4. Conclusions

The preloading technique proposed in the present study was viable for loading HOCs to PDMS disks, especially for HHOCs. Partition coefficients of HOCs with a wide range of hydrophobicity were measured using preloaded PDMS disks and followed the orders of  $K_{\text{SL,PDMS}} > K_{\text{ML,PDMS}} > K_{\text{pro,PDMS}}$ . The values were relatively constant for HOCs with  $K_{\text{OW}}$  values over six orders of magnitude, ensuring the application of PDMS-based samplers for assessing bioaccumulation potential of HHOCs. The divergence of  $K_{\text{PDMS,pro}}$  obtained by the uptake and depletion methods was explained by slow diffusion of HHOCs in PDMS because of their large molecular size. When using PDMS measurements to predict HOC bioaccumulation in organism, it is recommended to take all biological phases (SL, ML and protein) into consideration.

## Acknowledgements

This work was supported by the National Science Foundation of China (41473106 and 41503091), Guangdong Provincial Department of Science and Technology (2015TX01Z168) and the Natural Science Foundation of Guangdong Province, China (2015A030310219 and 2016A030312009). This is contribution No. IS-2384 from GIGCAS.

## Appendix A. Supplementary data

Supplementary data to this article can be found online at <http://dx.doi.org/10.1016/j.scitotenv.2017.04.123>.

## References

- Allan, I.J., Bæk, K., Haugen, T.O., Hawley, K.L., Høgfjeldt, A.S., Lillicrap, A.D., 2013. In vivo passive sampling of nonpolar contaminants in brown trout (*Salmo trutta*). *Environ. Sci. Technol.* 47, 11660–11667.
- Booij, K., Robinson, C.D., Burgess, R.M., Mayer, P., Roberts, C.A., Ahrens, L., Allan, I.J., Brant, J., Jones, L., Kraus, U.R., Larsen, M.M., Lepom, P., Petersen, J., Proefrock, D., Roose, P., Schäfer, S., Smedes, F., Tixier, C., Vorkamp, K., Whitehouse, P., 2015. Passive sampling in regulatory chemical monitoring of nonpolar organic compounds in the aquatic environment. *Environ. Sci. Technol.* 50, 3–17.
- Brennan, A.A., Harwood, A.D., You, J., Landrum, P.F., Lydy, M.J., 2009. Degradation of fipronil in anaerobic sediments and the effect on porewater concentrations. *Chemosphere* 77, 22–28.
- Brown, R.S., Akhtar, P., Åkerman, J., Hampel, L., Kozin, I.S., Villerius, L.A., Klammer, H.J.C., 2001. Partition controlled delivery of hydrophobic substances in toxicity tests using poly(dimethylsiloxane) (PDMS) films. *Environ. Sci. Technol.* 35, 4097–4102.
- de Bruyn, A.M.H., Gobas, F.A.P.C., 2007. The sorptive capacity of animal protein. *Environ. Toxicol. Chem.* 26, 1803–1808.
- Di Filippo, E.L., Eganhouse, R.P., 2010. Assessment of PDMS-water partition coefficients: implications for passive environmental sampling of hydrophobic organic compounds. *Environ. Sci. Technol.* 44, 6917–6925.
- Diamond, M.L., Melymuk, L., Csiszar, S.A., Robson, M., 2010. Estimation of PCB stocks, emissions, and urban fate: will our policies reduce concentrations and exposure? *Environ. Sci. Technol.* 44, 2777–2783.

- Elissen, H.J.H., Mulder, W.J., Hendrickx, T.L.G., Elbersen, H.W., Beelen, B., Temmink, H., Buisman, C.J.N., 2010. Aquatic worms grown on biosolids: biomass composition and potential applications. *Bioresour. Technol.* 101, 804–811.
- Endo, S., Bauerfeind, J., Goss, K.-U., 2012. Partitioning of neutral organic compounds to structural proteins. *Environ. Sci. Technol.* 46, 12697–12703.
- Endo, S., Escher, B.I., Goss, K.-U., 2011. Capacities of membrane lipids to accumulate neutral organic chemicals. *Environ. Sci. Technol.* 45, 5912–5921.
- Endo, S., Goss, K.-U., 2011. Serum albumin binding of structurally diverse neutral organic compounds: data and models. *Chem. Res. Toxicol.* 24, 2293–2301.
- Endo, S., Mewburn, B., Escher, B.I., 2013. Liposome and protein–water partitioning of polybrominated diphenyl ethers (PBDEs). *Chemosphere* 90, 505–511.
- Escher, B.I., Cowan-Ellsberry, C.E., Dyer, S., Embry, M.R., Erhardt, S., Halder, M., Kwon, J.-H., Johanning, K., Oosterwijk, M.T.T., Rutishauser, S., Segner, H., Nichols, J., 2011. Protein and lipid binding parameters in rainbow trout (*Oncorhynchus mykiss*) blood and liver fractions to extrapolate from an in vitro metabolic degradation assay to in vivo bioaccumulation potential of hydrophobic organic chemicals. *Chem. Res. Toxicol.* 24, 1134–1143.
- Escher, B.I., Schwarzenbach, R.P., 2002. Mechanistic studies on baseline toxicity and uncoupling of organic compounds as a basis for modeling effective membrane concentrations in aquatic organisms. *Aquat. Sci.* 64, 20–35.
- Geisler, A., Endo, S., Goss, K.-U., 2012. Partitioning of organic chemicals to storage lipids: elucidating the dependence on fatty acid composition and temperature. *Environ. Sci. Technol.* 46, 9519–9524.
- Grant, S., Schacht, V.J., Escher, B.I., Hawker, D.W., Gaus, C., 2016. Experimental solubility approach to determine PDMS–water partition constants and PDMS activity coefficients. *Environ. Sci. Technol.* 50, 3047–3054.
- van der Heijden, S.A., Hermens, J.L.M., Sinnige, T.L., Mayer, P., Gilbert, D., Jonker, M.T.O., 2015. Determining high-quality critical body residues for multiple species and chemicals by applying improved experimental design and data interpretation concepts. *Environ. Sci. Technol.* 49, 1879–1887.
- Hites, R.A., 2004. Polybrominated diphenyl ethers in the environment and in people: a meta-analysis of concentrations. *Environ. Sci. Technol.* 38, 945–956.
- Jahnke, A., MacLeod, M., Wickstrom, H., Mayer, P., 2014a. Equilibrium sampling to determine the thermodynamic potential for bioaccumulation of persistent organic pollutants from sediment. *Environ. Sci. Technol.* 48, 11352–11359.
- Jahnke, A., Mayer, P., McLachlan, M.S., 2012. Sensitive equilibrium sampling to study polychlorinated biphenyl disposition in baltic sea sediment. *Environ. Sci. Technol.* 46, 10114–10122.
- Jahnke, A., Mayer, P., McLachlan, M.S., Wickstrom, H., Gilbert, D., MacLeod, M., 2014b. Silicone passive equilibrium samplers as 'chemometers' in eels and sediments of a Swedish lake. *Environ. Sci. Process. Impacts* 16, 464–472.
- Jahnke, A., Mayer, P., Schäfer, S., Witt, G., Haase, N., Escher, B.I., 2016. Strategies for transferring mixtures of organic contaminants from aquatic environments into bioassays. *Environ. Sci. Technol.* 50, 5424–5431.
- Jahnke, A., McLachlan, M.S., Mayer, P., 2008. Equilibrium sampling: partitioning of organochlorine compounds from lipids into polydimethylsiloxane. *Chemosphere* 73, 1575–1581.
- Jin, L., Gaus, C., van Mourik, L., Escher, B.I., 2013. Applicability of passive sampling to bioanalytical screening of bioaccumulative chemicals in marine wildlife. *Environ. Sci. Technol.* 47, 7982–7988.
- Klosterhaus, S.L., Dreis, E., Baker, J.E., 2011. Bioaccumulation kinetics of polybrominated diphenyl ethers from estuarine sediments to the marine polychaete, *Nereis virens*. *Environ. Toxicol. Chem.* 30, 1204–1212.
- Li, H.Z., Zhang, B.Z., Wei, Y.L., Wang, F., Lydy, M.J., You, J., 2014. Bioaccumulation of highly hydrophobic organohalogen flame retardants from sediments: application of toxicokinetics and passive sampling techniques. *Environ. Sci. Technol.* 48, 6957–6964.
- Lohmann, R., Muir, D., Zeng, E.Y., Bao, L.J., Allan, I.J., Arinaitwe, K., Booij, K., Helm, P., Kaserzon, S., Mueller, J.F., Shibata, Y., Smedes, F., Tzapakis, M., Wong, C.S., You, J., 2017. Aquatic Global Passive Sampling (AQUA-GAPS) revisited: first steps toward a network of networks for monitoring organic contaminants in the aquatic environment. *Environ. Sci. Technol.* 51, 1060–1067.
- Mäenpää, K., Leppänen, M.T., Figueiredo, K., Mayer, P., Gilbert, D., Jahnke, A., Gil-Allué, C., Akkanen, J., Nybom, I., Herve, S., 2015b. Fate of polychlorinated biphenyls in a contaminated lake ecosystem: combining equilibrium passive sampling of sediment and water with total concentration measurements of biota. *Environ. Toxicol. Chem.* 34, 2463–2474.
- Mäenpää, K., Leppänen, M., Figueiredo, K., Tigistu-Sahle, F., Käkelä, R., 2015a. Sorptive capacity of membrane lipids, storage lipids, and proteins: a preliminary study of partitioning of organochlorines in lean fish from a PCB-contaminated freshwater lake. *Arch. Environ. Contam. Toxicol.* 68, 193–203.
- Mäenpää, K., Leppänen, M.T., Reichenberg, F., Figueiredo, K., Mayer, P., 2011. Equilibrium sampling of persistent and bioaccumulative compounds in soil and sediment: comparison of two approaches to determine equilibrium partitioning concentrations in lipids. *Environ. Sci. Technol.* 45, 1041–1047.
- Mayer, P., Parkerton, T.F., Adams, R.G., Cargill, J.G., Gan, J., Gouin, T., Gschwend, P.M., Hawthorne, S.B., Helm, P., Witt, G., You, J., Escher, B.I., 2014. Passive sampling methods for contaminated sediments: scientific rationale supporting use of freely dissolved concentrations. *Integr. Environ. Assess. Manag.* 10, 197–209.
- Muijs, B., Jonker, M.T.O., 2009. Temperature-dependent bioaccumulation of polycyclic aromatic hydrocarbons. *Environ. Sci. Technol.* 43, 4517–4523.
- Quinn, C.L., van der Heijden, S.A., Wania, F., Jonker, M.T.O., 2014. Partitioning of polychlorinated biphenyls into human cells and adipose tissues: evaluation of octanol, triolein, and liposomes as surrogates. *Environ. Sci. Technol.* 48, 5920–5928.
- Rusina, T.P., Smedes, F., Klanova, J., 2010. Diffusion coefficients of polychlorinated biphenyls and polycyclic aromatic hydrocarbons in polydimethylsiloxane and low-density polyethylene polymers. *J. Appl. Polym. Sci.* 116, 1803–1810.
- Rusina, T.P., Smedes, F., Klanova, J., Booij, K., Holoubek, I., 2007. Polymer selection for passive sampling: a comparison of critical properties. *Chemosphere* 68, 1344–1351.
- Schäfer, S., Antoni, C., Möhlenkamp, C., Claus, E., Reifferscheid, G., Heining, P., Mayer, P., 2015. Equilibrium sampling of polychlorinated biphenyls in River Elbe sediments - linking bioaccumulation in fish to sediment contamination. *Chemosphere* 138, 856–862.
- Sun, R.X., Luo, X.J., Tang, B., Li, Z.R., Wang, T., Tao, L., Mai, B.X., 2016. Persistent halogenated compounds in fish from rivers in the Pearl River Delta, South China: geographical pattern and implications for anthropogenic effects on the environment. *Environ. Res.* 146, 371–378.
- Valderrama, J.F.N., Baek, K., Molina, F.J., Allan, I.J., 2016. Implications of observed PBDE diffusion coefficients in low density polyethylene and silicone rubber. *Environ. Sci. Process. Impacts* 18, 87–94.
- Wang, P., Zhang, Q.H., Zhang, H.D., Wang, T., Sun, H.Z., Zheng, S.C., Li, Y.M., Liang, Y., Jiang, G.B., 2016. Sources and environmental behaviors of Dechlorane Plus and related compounds - a review. *Environ. Int.* 88, 206–220.
- Xie, M., Yang, Z.Y., Bao, L.J., Zeng, E.Y., 2009. Equilibrium and kinetic solid-phase microextraction determination of the partition coefficients between polychlorinated biphenyl congeners and dissolved humic acid. *J. Chromatogr. A* 1216, 4553–4559.
- Yang, Z.Y., Zhao, Y.Y., Tao, F.M., Ran, Y., Mai, B.X., Zeng, E.Y., 2007. Physical origin for the nonlinear sorption of very hydrophobic organic chemicals in a membrane-like polymer film. *Chemosphere* 69, 1518–1524.
- You, J., Landrum, P.F., Trimble, T.A., Lydy, M.J., 2007. Availability of polychlorinated biphenyls in field-contaminated sediment. *Environ. Toxicol. Chem.* 26, 1940–1948.
- Yu, G., Bu, Q.W., Cao, Z.G., Du, X.M., Xia, J., Wu, M., Huang, J., 2016. Brominated flame retardants (BFRs): a review on environmental contamination in China. *Chemosphere* 150, 479–490.
- Zhang, B.Z., Li, H.Z., Wei, Y.L., You, J., 2013. Bioaccumulation kinetics of polybrominated diphenyl ethers and decabromodiphenyl ethane from field-collected sediment in the oligochaete, *Lumbricus variegatus*. *Environ. Toxicol. Chem.* 32, 2711–2718.